A Robotic Assistance Personalization Control Approach of Hip Exoskeletons for Gait Symmetry Improvement

Qiang Zhang¹, Xikai Tu², Jennie Si³, Michael D. Lewek⁴, and He (Helen) Huang^{1*}

Abstract—Healthy human locomotion functions with good gait symmetry depend on rhythmic coordination of the left and right legs, which can be deteriorated by neurological disorders like stroke and spinal cord injury. Powered exoskeletons are promising devices to improve impaired people's locomotion functions, like gait symmetry. However, given higher uncertainties and the time-varying nature of human-robot interaction, providing personalized robotic assistance from exoskeletons to achieve the best gait symmetry is challenging, especially for people with neurological disorders. In this paper, we propose a hierarchical control framework for a bilateral hip exoskeleton to provide the adaptive optimal hip joint assistance with a control objective of imposing the desired gait symmetry during walking. Three control levels are included in the hierarchical framework, including the high-level control to tune three control parameters based on a policy iteration reinforcement learning approach, the middle-level control to define the desired assistive torque profile based on a delayed output feedback control method, and the low-level control to achieve a good torque trajectory tracking performance. To evaluate the feasibility of the proposed control framework, five healthy young participants are recruited for treadmill walking experiments, where an artificial gait asymmetry is imitated as the hemiparesis post-stroke, and only the 'paretic' hip joint is controlled with the proposed framework. The pilot experimental studies demonstrate that the hierarchical control framework for the hip exoskeleton successfully (asymmetry index from 8.8% to -0.5%) and efficiently (less than 4 minutes) achieved the desired gait symmetry by providing adaptive optimal assistance on the 'paretic' hip joint.

I. INTRODUCTION

Over the last two decades, there has been a flurry of research efforts in developing wearable lower-limb exoskeletons to augment functions for healthy individuals [1], [2] or provide rehabilitation/assistance for individuals with motor deficits [3], [4]. Focusing on the hip joint, various powered joint configurations, actuator designs, and control techniques have been reported to assist gait rehabilitation and human performance augmentation [5]–[9]. The rising research interest on hip exoskeletons lies in 1) the hip is important for

*This work was partly supported by National Institute on Disability, Independent Living, and Rehabilitation Research #90ARHF0004 and #90REGE0017, National Institutes of Health #R21HD098570, and National Science Foundation #2211739, #2211740, #1926998, and #1808752. Corresponding author: He Huang (hhuang11@ncsu.edu).

powering upright locomotion and postural control [10], 2) the hip joint is capable of manipulating step length, step width, and associated gait symmetry during walking, 3) compared with the ankle joint, the hip joint needs higher metabolic cost for the generation of similar mechanical joint power owing to the differences in muscle characteristics [11], and 4) compared with ankle/knee exoskeletons, hip exoskeletons add less mass to the leg, altering the leg dynamics to a lesser degree. Typically, individuals with neurological disorders caused by diseases or injuries such as a stroke and spinal cord injury generally have muscle weakness, which could lead to insufficient force or torque at the hip joints during locomotion [12], which easily causes gait asymmetry, increase metabolic cost, and poor balance control [13] that deteriorate activities of daily living. Therefore, improving gait symmetry is significant for individuals with neurological impairments.

Many recent research studies have addressed gait symmetry improvement by using hip exoskeletons and three main approaches, including joint trajectory-tracking control [14], [15], finite-state-machine (FSM)-based assistive control [16], [17], and adaptive frequency oscillators (AFO)-based assistive control [18]-[21]. However, the trajectory-tracking position control may cause discomfort or even injuries to patient wearers who still have voluntary motor functions although it is more appropriate for patient wearers with full paraplegia, which potentially discourages active engagement of the patients. In addition, most of the above studies utilize the fixed and pre-defined assistance torque/force profiles combined with discrete walking gait phases or continuous gait phase detection or human motion intent to provide hip joint assistance [22]. The discrete walking gait phases or continuous gait phase detection usually depends on the ground reaction force (GRF) or insole force sensing resistor (FSR) measurements, which typically increase the complexity of the human-exoskeleton interaction system. Lim et al. [22] proposed a delayed output feedback control method for a hip exoskeleton to assist walking functions, where the assistive level is determined by the scale gain of the orthogonal function difference between both joints' trajectories and a time delay factor. Although it did not require additional gait phase detection or human motion intent, control parameters were still fixed for inter-subject experiments.

Patients with neurological disorders, like stroke, present large variations in gait impairment and gait pattern [23], [24]. This considerable inter-human variation emphasizes the importance of customizing the robotic assistance on the impaired hip joint, thus optimizing the user's gait symmetry

¹Q. Zhang and H. Huang are with the Joint Department of Biomedical Engineering, North Carolina State University and the University of North Carolina at Chapel Hill, Raleigh, NC 27695 USA.

²X. Tu is with the Department of Mechanical Engineering, Hubei University of Technology, Wuhan, Hubei, 430068 China.

³J. Si is with the Department of Electrical, Computer, and Energy Engineering, Arizona State University, Tempe, AZ 85281 USA.

⁴M. Lewek is with the Department of Allied Health Sciences, The University of North Carolina at Chapel Hill, Chapel Hill, NC 27599, USA.

improvement. To provide personalized robotic optimal assistance (OA), recent studies have developed new concepts and automatic engineering approaches, of which two representative ones are human-in-the-loop (HIL) optimization approaches [25]-[31] and reinforcement learning (RL) approaches [32]–[35]. Specifically related to hip exoskeletons, Ding et al. [29] proposed to use a Bayesian optimization approach to tune the shape parameters of the hip extension assistive torque for a wearable hip exosuit with a control goal of minimizing human metabolic rate during walking. Considering the same control goal, Gordon et al. [36] developed a musculoskeletal model-based online metabolic rate estimation, which was combined with a Bayesian optimization approach to tune the shape parameters of the hip flexionextension assistive torque. Tu et al. [34] and Zhang et al. [35] proposed to implement a least square policy iteration (LSPI)based RL control framework to tune the shape parameters of the hip extension and hip extension-flexion assistive torque profiles, with the control goals of maximizing the transferred power and imposing targeted hip joint trajectory, respectively.

Although the aforementioned approaches have demonstrated the promising performance of automatic control parameters tuning of exoskeletons, very few studies have focused on maximizing gait symmetry by providing adaptive optimal assistance from hip exoskeletons [37]. Given the fact that people with motor impairments usually have limited capability for a long time walking, can we personalize the robotic assistance control fast for clinical applications? To address this critical challenge, in this study, we proposed a hierarchical control framework to optimally personalize robotic assistance on the hip joint with a control objective of achieving desired/reference gait symmetry. There are three control levels, where the high-level control is to tune control parameters according to a policy iteration RL approach; the middle-level control is to define the desired robotic assistance torque profile based on a delayed output feedback control (DOFC) approach; and the lowlevel control is to achieve a good torque trajectory tracking performance. To demonstrate the feasibility of the proposed control framework for impaired individuals post-stroke, we designed a scenario-equivalent study on unimpaired human subjects with artificial imitation of hemiparesis post-stroke. The main contributions of this study include 1) the dimension reduction of tunable control parameters for providing both hip flexion and extension assistance when compared to [35], [38]; 2) the online inter-leg coordination-based assistance torque profile generation; 3) the consideration of both gait symmetry and control parameters increment as components of the cost function, 4) the time-efficient control parameters tuning procedure, and 5) the potential GRF- or FSR-free implementations for daily locomotion tasks.

II. METHODS

The control framework design with three levels in this study is shown in Fig. 1 and more details are given below.

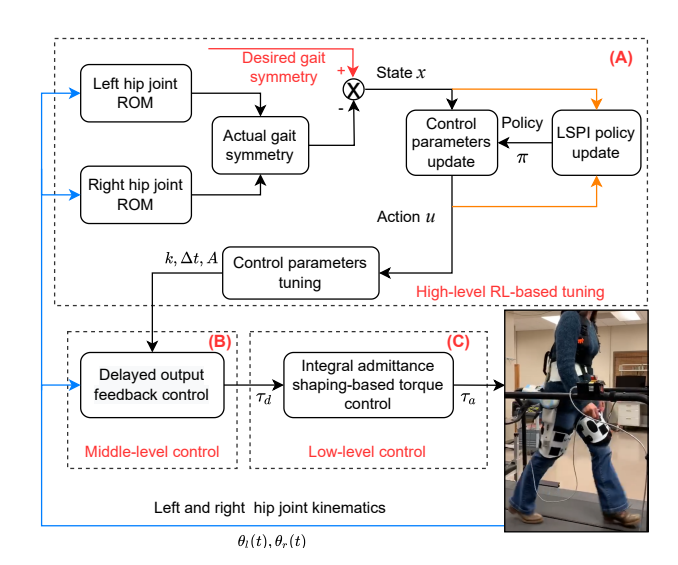


Fig. 1. The hierarchical control framework that enables the personalization of hip exoskeleton assistance to walk. (A) The high-level RL-based control learns to personalize control parameters. (B) The middle-level delayed output feedback control during walking generates the desired torque profile. (C) The low-level intrinsic torque controller tracks desired assistive torque generated from the middle-level control.

A. Problem formulation & middle-/low-level control design

Individuals with hemiparesis following post-stroke usually exhibit weakness in local lower-limb joints, like the limited motion of the right hip joint shown in Fig. 2 (a). Compared to the unimpaired hip joint, although the motion amplitude of the impaired hip joint is constrained, its cyclic motion pattern and cadence are still maintained similarly to the unimpaired side. Individuals with hemiparesis are more vulnerable to external disturbances, so a slight mismatch between their intended motion and the robotic assistance can be fatal. To compensate for the limited motion of the impaired hip joint while considering the motion coordination between bilateral hip joints, an further modified intuitive middle-level delayed output feedback controller (DOFC) that directly responds to the wearer's hip joint motion patterns, proposed initially in [22], is applied here. As shown in Fig. 1 (B), this middlelevel control will facilitate a unified assistance design for the impaired hip joint but require customized control parameters to achieve the best gait symmetry.

Assume the impaired (right side) and unimpaired (left side) hip joint trajectories are represented by $\theta_r(t)$ and $\theta_l(t)$, respectively, the intermediate output feedback signal y(t) that represents the projected hip motion is given as

$$y(t) = \sin(\theta_r(t)) - \sin(\theta_l(t)). \tag{1}$$

Then the assistance torque for the impaired hip joint $\tau_d(t)$ will be generated through a combination of appropriate time delays Δt , a control amplification gain k, and a vertical shift gain A as

$$\tau_d(t) = k * y(t - \Delta t) + A. \tag{2}$$

Here, the three tunable parameters k, Δt , and A are adjusted according to the RL-based high-level control. To ensure walking stability and avoid potential adverse effects, the

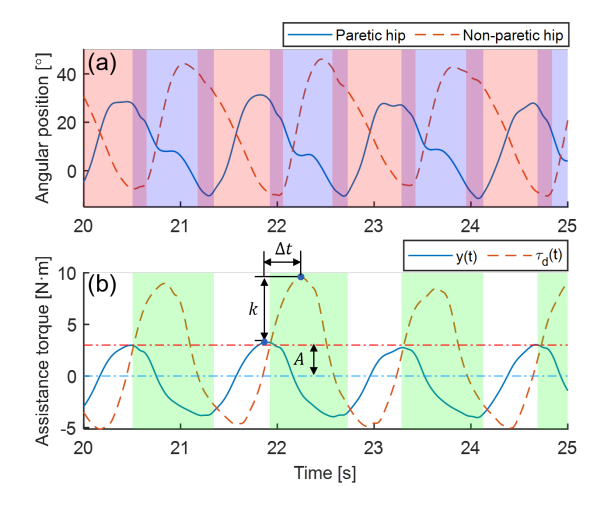


Fig. 2. (a) Typical non-paretic (red) and paretic (blue) hip joint trajectories during walking of people with hemiparesis following post-stroke. The red or blue regions represent the walking stance phases of the non-paretic and paretic sides, while the purple regions represent the double support phases. (b) The desired assistance torque generation on the paretic hip joint, where green regions represent the walking stance phases.

adjustment ranges for these three parameters are set as $k \in [0, 15] N \cdot m$, $\Delta t \in [0, 0.4]$ seconds, and $A \in [-5, 5] N \cdot m$, respectively. By adding the supplementary assistance torque to the biological torque of the paretic hip joint, the expected roll output would be an increased extension and flexion peak values, thus increasing the range of motion (ROM) on the paretic hip joint, which leads to a better gait symmetry.

At the low-level control, as shown in Fig. 1 (C), an intrinsic integral admittance shaping-based closed-loop torque control, as detailed in [34], [39], is applied, which is capable of achieving good torque tracking performance of the modular actuation unit of the hip exoskeleton during the dynamic locomotion tasks. For the motor itself, the closed-loop velocity control is used, where input signals include the position error (between the admittance reference position and real joint position) and admittance reference velocity, while the output signal is the real joint velocity. The stiffness and damping parameters in the low-level control are adjusted to ensure the near 1:1 scale-up of the sensitivity function.

B. RL-based high-level control design

As shown in Fig. 1 (A), we consider achieving the best ROM-associated gait symmetry as the control objective through RL-based automatic tuning of three control parameters in (2). The definition of gait symmetry is given as:

$$GS = (ROM_{UI} - ROM_I)/(2*(ROM_{UI} + ROM_I)), \quad (3)$$

where ROM_{UI} and ROM_I represent the ROM of the unimpaired and impaired hip joints, which is defined as the difference between the peak flexion and peak extension. Compared to other gait parameters (such as step length, stance time, etc.)-associated gait symmetry calculation, the main advantage of the ROM-associated gait symmetry is that it only requires onboard encoders measurement, which is

beneficial for avoiding extra sensors and maximizing the exoskeleton's portability. Assuming the desired gait symmetry as GS_d , the state variable, $x \in \mathbb{R}$, is formulated according to the differences between the desired and real gait symmetry variables as $x = GS - GS_d$.

To formulate the RL control solution for assistive torque control parameters tuning, we consider the human-hip exoskeleton system as a discrete-time dynamic model

$$x(n+1) = f(x(n), u(n)),u(n) = h(x(n)), n = 0, 1, 2...$$
 (4)

where n represents the discrete time index (measurement sample) in iterative control updates, $f(\cdot, \cdot)$ represents the transition function that maps state and action variables at the current measurement sample to the upcoming state variable, and $h(\cdot)$ represents the corresponding tuning policy that determines the action variables according to the current state variable. The domain of $f(\cdot,\cdot)$ is denoted as $\mathscr{D} \triangleq$ $(x, u)|x \in \mathcal{X}, u \in \mathcal{U}$, where \mathcal{X} and \mathcal{U} are compact sets with dimensions of 1 and 3, respectively. In this study, control parameters are updated every four consecutive gait cycles, within which state variables are calculated and averaged across gait cycles after applying low-pass filtering to realtime hip joint trajectory measurements. The tuning policy his updated every 20 measurement samples (80 gait cycles). Each measurement sample is considered as four consecutive gait cycles. During the n^{th} sample, the control action $u(n) \in$ \mathbb{R}^3 is defined as $u(n) = [\delta k(n), \delta \Delta t(n), \delta A(n)]^T$. The initial control parameters of k(0), $\Delta t(0)$, and A(0) are selected randomly within the aforementioned ranges and conditions.

The temporal control performance is assessed iteratively by defining the stage cost at the measurement sample index n in a quadratic form

$$r(x(n), u(n)) = x^{T}(n)M_{x}x(n) + u^{T}(n)M_{u}u(n),$$
 (5)

where $M_x \in \mathbb{R}$ and $M_u \in \mathbb{R}^{3 \times 3}$ are all positive definite weighting matrices. Given a deterministic policy $h^{(i)}$ $(i = \lfloor n/20 \rfloor)$, the state-action value function (Q-function) $Q^{h^{(i)}}$ is defined across all possible state and action variables. The Q-function of a policy $h^{(i)}$ indicates the expected and discounted total cost when taking action u(n) in the state x(n), thereafter [40]

$$Q^{h^{(i)}}(n) = r(x(n), u(n)) + \sum_{t=n+1}^{\infty} \gamma^{t-n} r(x(n), u(n))$$
$$= r(x(n), u(n)) + \gamma Q^{h^{(i)}}(x(n+1), u(n+1)), \quad (6)$$

where γ is the discount factor. The goal of RL control is to acquire an optimal policy, h^* , that will be used to minimize the Q-function, noted as $Q^*(x(n), u(n))$, as below

$$Q^{*}(n) = \min_{h} Q^{h^{(i)}}(x(n), u(n))$$

$$= r(x(n), u(n)) + \gamma \min_{u(n+1)} Q^{h^{(i+1)}}(x(n+1), u(n+1))$$

$$= r(x(n), u(n)) + \gamma Q^{*}(x(n+1), h^{*}(x(n+1))). \quad (7)$$

During each iteration, the *policy evaluation* step computes the Q-function $Q^{h^{(i)}}$ by solving the Bellman equation

approximately and the *policy improvement* step defines the improved greedy policy $h^{(i+1)}$ over $Q^{h^{(i)}}$ as

$$h^{(i+1)}(x(n)) = \underset{u(n)}{\arg\min} Q^{h^{(i)}}(n), \tag{8}$$

where u(n) is selected from the admissible compact set \mathcal{U} . By using the quadratic basis functions (QBFs), *policy improvement* step is equivalent to solving a quadratic programming problem. Therefore, the policy $h^{(i+1)}$ is at least as good as $h^{(i)}$, if not better. The two steps are repeated until there is no change in the policy, thus reaching the optimal policy h^* .

C. Solution for online LSPI with policy approximation

In conventional LSPI, Q-functions are approximated by using a linear parameterization as

$$\hat{Q}(x(n), u(n)) = \phi^{T}(x(n), u(n))\theta, \tag{9}$$

where $\phi^{(}x(n), u(n)) \in \mathbb{R}^{N}$ is a vector of N QBFs and $\theta \in \mathbb{R}^{N}$ is a parameter vector. Similar to existing model-free LSPI-based RL approaches [34], [35], [40]–[43] that do not depend on the exact model knowledge about the controlled system or the optimal solution, we applied no prior knowledge about the optimal policy or more generally about good policies to address the personalization problem, called online LSPI with policy approximation [44]. Consider a linearly parameterized policy

$$\hat{h}(x(n)) = \boldsymbol{\psi}^{T}(x(n))\vartheta, \tag{10}$$

where $\psi(x(n)) = [\psi_1(x(n)), ..., \psi_{N_s}(x(n))]^T$ is a vector that contains N_s state-dependent quadratic basis functions, and ϑ is the policy parameter vector. Although a scalar action is assumed here, the parameterization can be easily extended to multiple action variables. If there is no available prior knowledge of the policy, approximate policy improvement can be performed by solving the unconstrained linear least square problem that is given by

$$\vartheta_{l+1} = \vartheta^*, \, \vartheta^* \in \underset{\vartheta}{\operatorname{arg\,min}} \sum_{n=1}^{Ns} (\psi^T(x(n))\vartheta - u(n)), \quad (11)$$

where $u(n) \in \arg\max \phi^T(x(n), u(n))\theta_l$. The parameter ϑ_{l+1} leads to a policy improvement, and $\{x(1), x(2), ..., x(N_s)\}$ is a set of samples to be used for policy improvement.

III. HUMAN-IN-THE-LOOP EXPERIMENTAL STUDY DESIGN AND IMPLEMENTATION

A. Human participants and experimental protocol

The treadmill walking protocol was approved by the Institutional Review Board (IRB) of the North Carolina State University (IRB approval number: 24671). Five young, healthy participants (mass: 73.9 ± 8.1 kg, height: 170.2 ± 3.7 cm, age: 26.6 ± 5.6 years old, identified as participants A01, A02,..., A05) without any neurological disorders were recruited in this study. All participants were familiarized with the experimental details and signed the consent form before any experimental studies. Each participant wore the bilateral

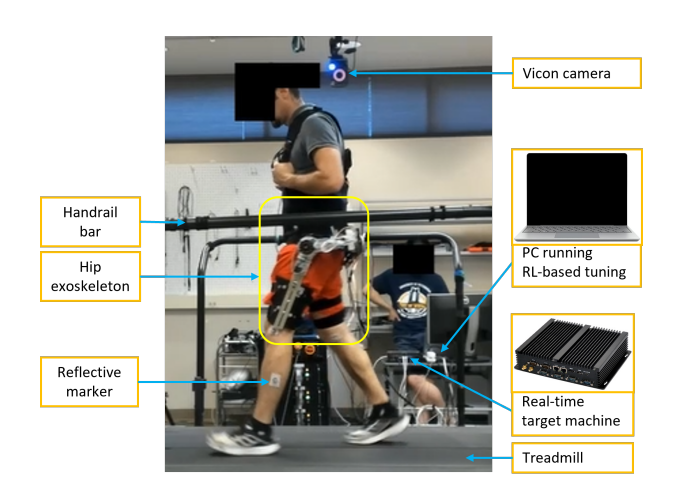


Fig. 3. Experimental setup of the walking task on the instrumented treadmill with the split belts.

hip exoskeleton and practiced walking in a transparent mode (zero assistance) on an instrumented treadmill (Bertec Corp., Columbus, OH, USA) at 1.0 m/s a day before the experimental sessions to ensure the participant felt comfortable walking with the exoskeleton.

Figure 3 presents the experimental setup, where participants wear a bilateral hip exoskeleton throughout walking experiments. The exoskeleton consists of two degrees of freedom for flexion/extension motion on two hip joints, and each one could provide a continuous output torque of 34 N·m, a peak torque of approximately 57 N·m, and an angular velocity of up to 300 °/s. Detailed design and corresponding characteristics of the hip exoskeleton can be referred to [34], [35]. Given the advantages of the bilateral configuration of the hip exoskeleton, separate assistance patterns can be applied to the left and right hip joints, which facilitates the rationale of generating artificial gait asymmetry for unimpaired human subjects. Each participant walked on the treadmill at 1.0 m/s under four different conditions, including (1) transparent mode/zero assistance on both hip joints (C1), (2) artificial gait asymmetry by adding consistent unilateral assistance on the left hip joint while the right hip joint remains unassisted (C2), (3) RLbased control parameters tuning on the right hip joint while keeping the consistent assistance on the left hip joint (C3), (4) Personalized assistance on the right hip joint after RLbased tuning while keeping the consistent assistance on the left hip joint (C4). Under C1, C2, and C4, each participant walked stably for 100 gait cycles separately. Under condition C3, an up to 25-minute RL-based control parameters tuning procedure was conducted on each participant. Breaks of 5 minutes or as needed were given to participants between two consecutive conditions or after 5 minutes of walking under condition C3 to avoid any fatigue.

B. Artificial gait asymmetry generation

To imitate the similar results of post-stroke patients that were reported in [45] with an average of 9% gait asymmetry, we added consistent unilateral assistance on a left hip joint to

introduce artificial gait asymmetry while the right hip joint remained unassisted under the walking condition C2. The consistent unilateral assistance was generated by using the finite-state-machine impedance control as

$$\tau_u(t) = k_p(\theta_l(t) - \theta_e) + k_d \dot{\theta}_l(t), \tag{12}$$

where k_p , k_d , and θ_e denote the stiffness, damping, and equilibrium position parameters during either hip extension or flexion phases, respectively.

C. Implementation of control parameters tuning

Under the walking condition C3, each human subject walked on the treadmill in the transparent mode for both hip joints during the first ten gait cycles. Then, the hip exoskeleton began to provide consistent assistance on the left hip joint and to tune these three parameters in (2) on the right hip joint according to RL control policies. The tuning goal was considered met when state and stage cost stayed within the stopping rules (± 0.02 for state value and 0.0005 for stage cost) for eight continuous iterations. If the stopping rules were satisfied within 10 minutes, the training procedure was deemed successful; otherwise, it was unsuccessful. The discount factor was set as 0.9, and weighting coefficients as mentioned in (5) were set as $M_x = 1.0$ and $M_u = \text{diag}([0.1, 1.0, 0.2])$.

The initial set of control parameters $(k = 2N \cdot m, \Delta t =$ $0.1 \, sec$, and $A = 0 \, N \cdot m$) and a pre-trained policy as the initial policy were applied for the RL-based online tuning procedures on all participants. To obtain the pre-trained policy, we included an experienced hip exoskeleton user for five independent training walking trials on the treadmill at 1.0 m/s. The initial policy for these five trials was pseudo-randomly generated, and the initial control parameters set was the same as above. Therefore, five pre-training trials were performed with different pseudo-random initial policies. The policy associated with the most recent successful trial was used as the initial policy for all recruited human participants. The RL-based control parameters tuning was implemented in MATLAB (R2020a, MathWorks, MA, USA) at 500 Hz, and the low-level admittance control of the hip exoskeleton operated in C++ at 1000 Hz. The user datagram protocol (UDP) was used for the data communication between the high- and middle-level control programs.

D. Data collection, processing, and analysis

The featured benefit of the DOFC is the independence of GRF when determining the desired hip joint assistance; therefore, GRF data was not required for the control parameters tuning under condition C3. We only collected GRF data at 1000 Hz from force plates (AMTI, Watertown, MA, USA) for post-processing and gait analysis purposes. During the control parameters tuning procedure via LSPI in C3, we recorded the iterative updates of all state variables, action variables, stage cost, and control parameters in every sample. During all walking conditions, besides GRF data, we simultaneously recorded onboard signals from the hip exoskeleton.

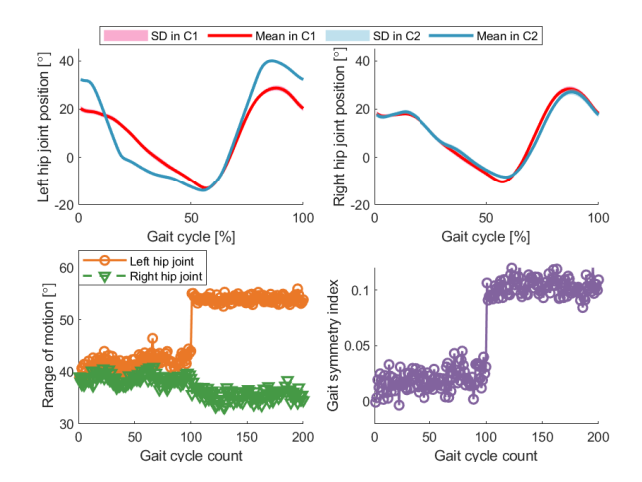


Fig. 4. Results of symmetry and asymmetric treadmill walking before and after adding consistent unilateral assistance under conditions C1 and C2. The top plots show the left and right hip joint trajectories vs. normalized gait cycle, while the bottom plots show the ROM of both hip joints vs. gait cycle counts and the gait symmetry index vs. gait cycle counts.

including angular position, velocity, assistance torque, interactive torque, assistance power, and motor current at 500 Hz in MATLAB. Both GRF data and onboard signals were low-pass filtered through a 4th-order Butterworth filter with a cut-off frequency of 10 Hz in the post-processing.

The mean and standard deviation (SD) values of the hip joint ROM-associated gait symmetry index were calculated across all gait cycles under conditions C1, C2, and C4. According to the Shapiro-Wilk parametric hypothesis test (significance level α =0.05), the data followed the normal distribution (p > 0.05). Therefore, we conducted a one-way repeated-measure analysis of variance (ANOVA) followed by Tukey's honestly significant difference tests to evaluate the effect across different conditions. The significant difference level was chosen as p < 0.05 for all statistical tests.

IV. RESULTS AND DISCUSSIONS

A. Artificial gait asymmetry outcomes

By applying the consistent unilateral assistance mode while the other hip joint remains unassisted, artificial gait asymmetry could be generated. The impedance parameters during in (12) were set as $k_p = 25 \, N \cdot m/rad$, $k_d = 0.1 \, N \cdot m/(rad \cdot s)$, $q_e = -0.2 \, rad$ for hip extension phase and $k_p = 25 \, N \cdot m/rad$, $k_d = 0.1 \, N \cdot m/(rad \cdot s)$, $q_e = 0.8 \, rad$ for hip flexion phase, respectively. Take one representative participant as an example, shown in Fig. 4, the left hip joint trajectory was modulated after adding assistance while the right hip joint remained almost the same trajectory. The left hip joint ROM was increased by around 12.2° while the right side was reduced by around 3.1°, indicating participants had some compensatory movements even though no assistance was added to the right side. Eventually, the unilateral assistance introduced an asymmetry of 10.1%.

B. Performance of automatic tuning based on RL

The results regarding iterative changes of stage cost values, state variables, and control parameters during the RL-base

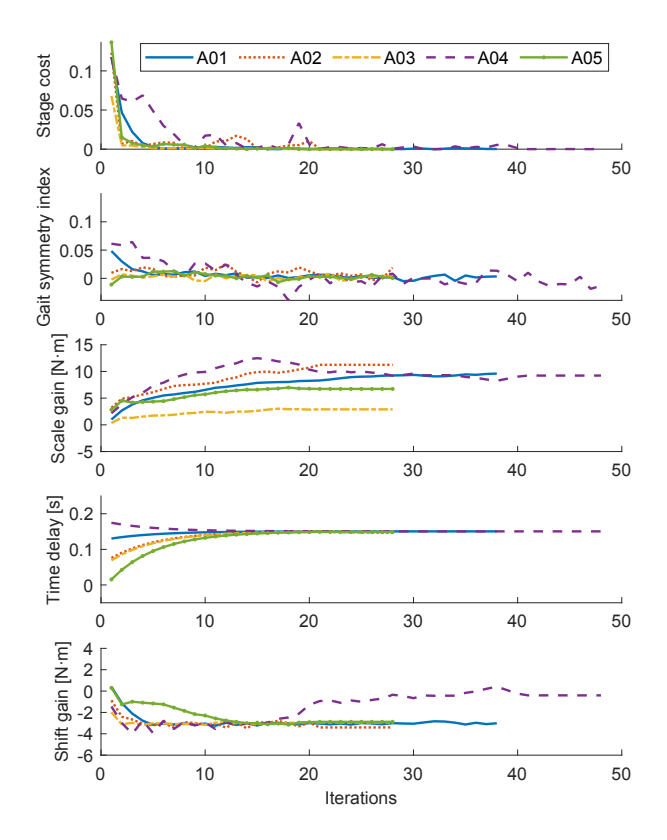


Fig. 5. Outcomes from the RL-based robotic assistance personalization procedure under condition C3 on all five participants, including iterative changes of stage cost, gait symmetry index, and control parameters. Each curve represents corresponding data from each participant.

Participant	Metrics at the stopping criteria				
	$k (N \cdot m)$	Δt (s)	$A (N \cdot m)$	Iteration	Time (s)
1	9.59	0.151	-3.01	38	178
2	11.24	0.147	-3.40	28	129
3	2.90	0.149	-2.94	28	135
4	9.23	0.150	-0.40	48	213
5	6.73	0.148	-2.88	28	139

tuning procedure under condition C3 are presented in Fig. 5, where each curve represents the data of each participant. It shows that the tuning duration varied from person to person, as the iteration numbers are 38, 28, 28, 48, and 28 for five participants. Correspondingly, the policy update numbers are 1, 1, 1, 2, and 1, respectively. Since the initial control parameters were fixed and not optimal for each participant, the state variable and reward values in the initial stages were relatively high, and eventually, both the state variable and stage cost converged within the thresholds aforementioned. The personalized control parameters when meeting stopping criteria, tuning iterations, and tuning time duration for all five participants are summarized in Table I.

It is noted that fixed impedance parameters in (12) were used to generate nearly consistent assistance on the left hip joint, which is supported by results in Fig. 6 that presents the

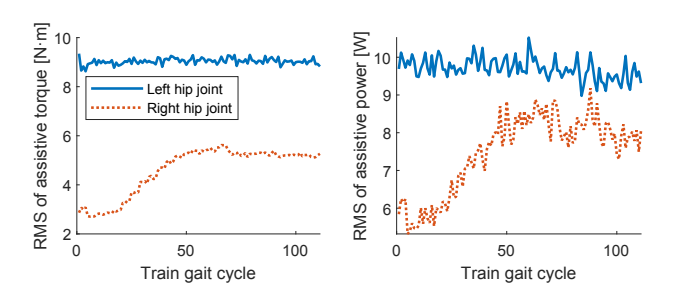


Fig. 6. Comparison results of gait cycle-normalized assistive torque and power root mean square (RMS) values on both hip joints of A05 under condition C3.

gait cycle-normalized assistance torque and power root mean square (RMS) values on both hip joints during the training procedure of participant A05. The torque/power variances for the left and right hip joints are $0.017 \ N \cdot m/0.077 \ W$ and $0.952 \ N \cdot m/1.048 \ W$, respectively, indicating the negligible variations of the assistance on the left hip joint.

C. Evaluation of personalized robotic assistance

Considering the control goal in this work is to regenerate the hip joint ROM-associated gait symmetry, we did not require the accurate joint trajectory matching between the left and right hip joints. In other words, the ROM match between hip joints was more critical than the sequential trajectory match. The relationship between the hip joint positions and velocities on both sides under conditions C1, C2, and C4 from a representative participant are presented in Fig. 7, where each curve represents averaged data across 100 gait cycles. The good trajectory match and ROM match between hip joints only occurred under condition C1, which implies high gait symmetry. After introducing gait asymmetry under condition C2, a significant ROM mismatch appeared, indicating both flexion and extension on the left hip joint were enhanced. After adding personalized optimal assistance under condition C4, the ROM match was regenerated as C1, but the trajectory mismatch remained. Similar joint kinematics results were also observed from other participants. Fig. 8 summarizes the gait symmetry results (mean \pm SD) across 100 gait cycles under conditions C1, C2, and C4 intrasubject and inter-subject. The gait symmetry index under C2 showed a significant increase when compared to C1 and C4; however, it did not show any significant difference between C1 and C4, both intra-subject and inter-subject. On average, the personalized optimal assistance in C4 effectively reduced the gait symmetry index from 8.8% to -0.5%. All significant difference levels are marked in Fig. 8.

The results of gait symmetry improvement in this study are comparable to or even better than the performance of existing lower-limb exoskeletons studies, such as from $21.5\%\pm3.3\%$ in artificially impaired condition to $3.4\%\pm0.5\%$ in assisted condition [21], from $11.1\%\pm0.7\%$ in artificially impaired condition to $3.9\%\pm0.6\%$ in assisted condition [46], and from 12.7% in artificially impaired condition to 7.4% in assisted condition [46]. More importantly, this study provides an adaptive optimal control framework to automatically tune

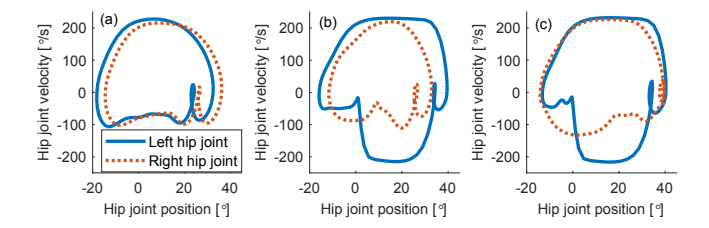


Fig. 7. Kinematics limit cycles on both hip joints under conditions C1 (a), C2 (b), and C4 (c). Data were averaged across 100 gait cycles under each condition on A05.

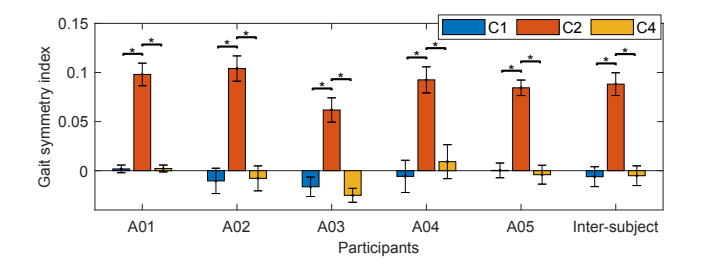


Fig. 8. ROM-associated gait symmetry results under conditions C1, C2, and C4. Individual data were averaged across 100 gait cycles under each condition. * represents the significant difference levels at p < 0.05.

control parameters for a hip exoskeleton to provide personalized optimal assistance that reproduces the desired gait symmetry. Compared to the approximate dynamic programmingbased adaptive control approach with one-dimensional control space in [37], we have a three-dimensional action space in this study, which could cause tuning efficiency issues by using the approach in [37]. As mentioned in previous evidence [44], [47], the policy iteration has the advantage of fast convergence over other classical RL algorithms, such as value iteration and gradient-based policy search (including the approximate dynamic programming). In this study, a total of three control parameters were efficiently tuned online to reach the optimal values individually between 2 to 4 minutes. Considering the variations from person to person, it is reasonable that personalized control parameters are different for different participants, as shown in Fig. 5 and Table I. According to [48], variations in the personalized control parameters after RL-based tuning emphasized the nature of the robotic assistance customization for an individual user to yield similar walking gait symmetry, which infers the necessity of assistance personalization.

This study is the first attempt to tune control parameters for wearable exoskeletons that can provide optimal gait function assistance but do not depend on gait phases or human motion intent detection, possibly opening a new avenue for the HIL optimization problem out of the laboratory and in real-world locomotion activities. Compared to existing HIL optimization approaches like in [25], [28]–[30], RL-based automatic control tuning has more time efficiency and can easily be scaled when meeting various walking conditions, like uneven terrain, speed change, or stairs [43]. More importantly, after tuning on one human participant under one condition, the optimal policy usually possesses higher

robustness and can be directly applied to the same walking condition on a new participant or a new walking condition on the same participant [43]. Although these preliminary results in the pilot study were promising, some limitations still exist. For example, the simulated spatial gait asymmetry on unimpaired human participants, where we assumed the enhanced side was the healthy side and the other side was the affected side, may not have the exact mechanism as gait asymmetry from people with motor impairments. Further investigation on other gait symmetry metrics, such as temporal and/or spatiotemporal symmetry will be necessary in future work. Then, we did not quantify the human adaptation to the varying robotic assistance given the short duration of the RL-based tuning. In addition, we did not address the systematic comparison between the proposed RL-based control approach and HIL optimization approaches, which will be interesting topics in future work.

V. CONCLUSION

In this work, we investigated a data-driven RL-based hierarchical control framework to provide personalized assistance from a hip exoskeleton, with the control objective of regenerating desired gait symmetry during walking. Three control levels were proposed to automatically tune three control parameters iteratively according to the least square policy iteration algorithm. Five young participants without neurological disorders were recruited to validate the effectiveness of the proposed control framework, where artificial gait asymmetry during walking was generated by applying consistent assistance mode on one hip joint, and the control parameters tuning was applied on the other hip joint. Humanin-the-loop experimental results during the tuning procedures demonstrated a fast convergence speed between 2 minutes and 4 minutes. Evaluation results illustrated that the control framework could provide optimal personalized assistance on the hip joint to drive the ROM-associated gait symmetry approaching the desired values. Our next step will focus on a more thorough evaluation of the proposed RL-based control framework on individuals with a chronic stroke while walking on the treadmill or overground.

REFERENCES

- A. B. Zoss, H. Kazerooni, and A. Chu, "Biomechanical design of the berkeley lower extremity exoskeleton (bleex)," *IEEE/ASME Trans. Mechatron.*, vol. 11, no. 2, pp. 128–138, 2006.
- [2] M. P. De Looze, T. Bosch, F. Krause, K. S. Stadler, and L. W. O'sullivan, "Exoskeletons for industrial application and their potential effects on physical work load," *Ergonomics*, vol. 59, no. 5, pp. 671–681, 2016.
- [3] J. L. Pons, "Rehabilitation exoskeletal robotics," *IEEE eng. med. biol. mag.*, vol. 29, no. 3, pp. 57–63, 2010.
- [4] D. Shi, W. Zhang, W. Zhang, and X. Ding, "A review on lower limb rehabilitation exoskeleton robots," *Chin. J. Mech. Eng.*, vol. 32, no. 1, pp. 1–11, 2019.
- [5] W. Huo, S. Mohammed, J. C. Moreno, and Y. Amirat, "Lower limb wearable robots for assistance and rehabilitation: A state of the art," *IEEE Syst. J.*, vol. 10, no. 3, pp. 1068–1081, 2014.
- [6] T. Yan, M. Cempini, C. M. Oddo, and N. Vitiello, "Review of assistive strategies in powered lower-limb orthoses and exoskeletons," *Robot. Auton. Syst.*, vol. 64, pp. 120–136, 2015.

- [7] A. J. Young and D. P. Ferris, "State of the art and future directions for lower limb robotic exoskeletons," *IEEE Trans. Neural Sys. Rehabil. Eng.*, vol. 25, no. 2, pp. 171–182, 2017.
- [8] B. Chen, B. Zi, L. Qin, and Q. Pan, "State-of-the-art research in robotic hip exoskeletons: A general review," *J. Orthop. Translat.*, vol. 20, pp. 4–13, 2020.
- [9] A. Rodríguez-Fernández, J. Lobo-Prat, and J. M. Font-Llagunes, "Systematic review on wearable lower-limb exoskeletons for gait training in neuromuscular impairments," *J. Neuroeng. Rehabil.*, vol. 18, no. 1, pp. 1–21, 2021.
- [10] D. J. Farris and G. S. Sawicki, "The mechanics and energetics of human walking and running: a joint level perspective," J. R. Soc. Interface., vol. 9, no. 66, pp. 110–118, 2012.
- [11] B. R. Umberger and J. Rubenson, "Understanding muscle energetics in locomotion: new modeling and experimental approaches," *Exerc. Sport Sci. Rev.*, vol. 39, no. 2, pp. 59–67, 2011.
- [12] S. J. Olney and C. Richards, "Hemiparetic gait following stroke. part i: Characteristics," *Gait & posture*, vol. 4, no. 2, pp. 136–148, 1996.
- [13] L. N. Awad, J. Bae, K. O'donnell, S. M. De Rossi, K. Hendron, L. H. Sloot, P. Kudzia, S. Allen, K. G. Holt, T. D. Ellis, et al., "A soft robotic exosuit improves walking in patients after stroke," Sci. Transl. Med., vol. 9, no. 400, p. eaai9084, 2017.
- [14] K. Suzuki, G. Mito, H. Kawamoto, Y. Hasegawa, and Y. Sankai, "Intention-based walking support for paraplegia patients with robot suit hal," Adv. Robot., vol. 21, no. 12, pp. 1441–1469, 2007.
- [15] R. Farris, H. Quintero, and M. Goldfarb, "Preliminary evaluation of a powered lower limb orthosis to aid walking in paraplegic individuals," *IEEE Trans. Neural Syst. Rehabil. Eng.*, vol. 19, no. 6, pp. 652–659, 2011
- [16] S. A. Murray, K. H. Ha, C. Hartigan, and M. Goldfarb, "An assistive control approach for a lower-limb exoskeleton to facilitate recovery of walking following stroke," *IEEE Trans. Neural Syst. Rehabil. Eng.*, vol. 23, no. 3, pp. 441–449, 2014.
- [17] J. Li, B. Shen, C.-M. Chew, C. L. Teo, and A. N. Poo, "Novel functional task-based gait assistance control of lower extremity assistive device for level walking," *IIEEE Trans. Ind. Electron.*, vol. 63, no. 2, pp. 1096–1106, 2015.
- [18] D. Zanotto, P. Stegall, and S. K. Agrawal, "Adaptive assist-as-needed controller to improve gait symmetry in robot-assisted gait training," in *IEEE international conference on robotics and automation (ICRA)*. IEEE, 2014, pp. 724–729.
- [19] K. Seo, J. Lee, Y. Lee, T. Ha, and Y. Shim, "Fully autonomous hip exoskeleton saves metabolic cost of walking," in *IEEE International* Conference on Robotics and Automation (ICRA). IEEE, 2016, pp. 4628–4635.
- [20] G. Aguirre-Ollinger, A. Narayan, and H. Yu, "Phase-synchronized assistive torque control for the correction of kinematic anomalies in the gait cycle," *IEEE Trans. Neural Syst. Rehabil. Eng.*, vol. 27, no. 11, pp. 2305–2314, 2019.
- [21] Y. Qian, H. Yu, and C. Fu, "Adaptive oscillator-based assistive torque control for gait asymmetry correction with a nsea-driven hip exoskeleton," *IEEE Trans. Neural Syst. Rehabil. Eng.*, vol. 30, pp. 2906–2915, 2022.
- [22] B. Lim, J. Lee, J. Jang, K. Kim, Y. J. Park, K. Seo, and Y. Shim, "Delayed output feedback control for gait assistance with a robotic hip exoskeleton," *IEEE Trans. Robot.*, vol. 35, no. 4, pp. 1055–1062, 2019.
- [23] S. Mulroy, J. Gronley, W. Weiss, C. Newsam, and J. Perry, "Use of cluster analysis for gait pattern classification of patients in the early and late recovery phases following stroke," *Gait & posture*, vol. 18, no. 1, pp. 114–125, 2003.
- [24] G. Kwakkel, B. Kollen, and E. Lindeman, "Understanding the pattern of functional recovery after stroke: facts and theories," *Restor. Neurol. Neurosci.*, vol. 22, no. 3-5, pp. 281–299, 2004.
- [25] D. Gopinath, S. Jain, and B. D. Argall, "Human-in-the-loop optimization of shared autonomy in assistive robotics," *IEEE Robot. Autom. Lett.*, vol. 2, no. 1, pp. 247–254, 2016.
- [26] J. R. Koller, D. H. Gates, D. P. Ferris, and C. D. Remy, "body-in-the-loop'optimization of assistive robotic devices: A validation study." in *Robotics: Science and Systems*, vol. 2016, 2016, pp. 1–10.
- [27] M. Kim, Y. Ding, P. Malcolm, J. Speeckaert, C. J. Siviy, C. J. Walsh, and S. Kuindersma, "Human-in-the-loop bayesian optimization of wearable device parameters," *PloS one*, vol. 12, no. 9, p. e0184054, 2017.

- [28] J. Zhang, P. Fiers, K. A. Witte, R. W. Jackson, K. L. Poggensee, C. G. Atkeson, and S. H. Collins, "Human-in-the-loop optimization of exoskeleton assistance during walking," *Science*, vol. 356, no. 6344, pp. 1280–1284, 2017.
- [29] Y. Ding, M. Kim, S. Kuindersma, and C. J. Walsh, "Human-in-the-loop optimization of hip assistance with a soft exosuit during walking," *Sci. Robot.*, vol. 3, no. 15, p. eaar5438, 2018.
- [30] J. Kim, G. Lee, R. Heimgartner, D. A. Revi, N. Karavas, D. Nathanson, I. Galiana, A. Eckert-Erdheim, P. Murphy, D. Perry, et al., "Reducing the metabolic rate of walking and running with a versatile, portable exosuit," *Science*, vol. 365, no. 6454, pp. 668–672, 2019.
- [31] S. Song and S. H. Collins, "Optimizing exoskeleton assistance for faster self-selected walking," *IEEE Trans. Neural Syst. Rehabil. Eng.*, vol. 29, pp. 786–795, 2021.
- [32] R. Huang, H. Cheng, J. Qiu, and J. Zhang, "Learning physical humanrobot interaction with coupled cooperative primitives for a lower exoskeleton," *IEEE Trans. Autom. Sci. Eng.*, vol. 16, no. 4, pp. 1566– 1574, 2019.
- [33] Y. Yuan, Z. Li, T. Zhao, and D. Gan, "Dmp-based motion generation for a walking exoskeleton robot using reinforcement learning," *IEEE Trans. Ind. Electron.*, vol. 67, no. 5, pp. 3830–3839, 2019.
- [34] X. Tu, M. Li, M. Liu, J. Si, and H. H. Huang, "A data-driven reinforcement learning solution framework for optimal and adaptive personalization of a hip exoskeleton," in *IEEE International Confer*ence on Robotics and Automation (ICRA), 2021, pp. 10610–10616.
- [35] Q. Zhang, V. Nalam, X. Tu, M. Li, J. Si, M. D. Lewek, and H. H. Huang, "Imposing healthy hip movement pattern and range by exoskeleton control for individualized assistance," *IEEE Robot. Autom. Lett.*, vol. 7, no. 4, pp. 11126–11133, 2022.
- [36] D. F. Gordon, C. McGreavy, A. Christou, and S. Vijayakumar, "Human-in-the-loop optimization of exoskeleton assistance via online simulation of metabolic cost," *IEEE Trans. Robot.*, vol. 38, no. 3, pp. 1410–1429, 2022.
- [37] T. Zhang, Y. Li, C. Ning, and B. Zeng, "Development and adaptive assistance control of the robotic hip exoskeleton to improve gait symmetry and restore normal gait," *IEEE Trans. Autom. Sci. Eng.*, 2022.
- [38] P. W. Franks, G. M. Bryan, R. M. Martin, R. Reyes, A. C. Lakmazaheri, and S. H. Collins, "Comparing optimized exoskeleton assistance of the hip, knee, and ankle in single and multi-joint configurations," *Wearable Technologies*, vol. 2, 2021.
- [39] U. Nagarajan, G. Aguirre-Ollinger, and A. Goswami, "Integral admittance shaping: A unified framework for active exoskeleton control," *Robot. Auton. Syst.*, vol. 75, pp. 310–324, 2016.
- [40] M. G. Lagoudakis and R. Parr, "Least-squares policy iteration," J. Mach. Learn. Res., vol. 4, pp. 1107–1149, 2003.
- [41] D. P. Bertsekas, "Approximate policy iteration: A survey and some new methods," *Int. J. Control. Theory Appl.*, vol. 9, no. 3, pp. 310– 335, 2011.
- [42] H. Yu, "Least squares temporal difference methods: An analysis under general conditions," SIAM J. Control Optim., vol. 50, no. 6, pp. 3310– 3343, 2012.
- [43] M. Li, Y. Wen, X. Gao, J. Si, and H. Huang, "Toward expedited impedance tuning of a robotic prosthesis for personalized gait assistance by reinforcement learning control," *IEEE Trans. Robot.*, vol. 38, no. 1, pp. 407–420, 2022.
- [44] L. Busoniu, R. Babuska, B. De Schutter, and D. Ernst, Reinforcement learning and dynamic programming using function approximators. CRC press, 2017.
- [45] K. K. Patterson, W. H. Gage, D. Brooks, S. E. Black, and W. E. McIlroy, "Changes in gait symmetry and velocity after stroke: a cross-sectional study from weeks to years after stroke," *Neurorehabil. Neural Repair*, vol. 24, no. 9, pp. 783–790, 2010.
- [46] G. Aguirre-Ollinger and H. Yu, "Lower-limb exoskeleton with variable-structure series elastic actuators: Phase-synchronized force control for gait asymmetry correction," *IEEE Trans. Robot.*, vol. 37, no. 3, pp. 763–779, 2020.
- [47] J. Si and Y.-T. Wang, "Online learning control by association and reinforcement," *IEEE Trans. Neural Netw.*, vol. 12, no. 2, pp. 264– 276, 2001.
- [48] Y. Wen, J. Si, A. Brandt, X. Gao, and H. H. Huang, "Online reinforcement learning control for the personalization of a robotic knee prosthesis," *IEEE Trans. Cybern.*, vol. 50, no. 6, pp. 2346–2356, 2019.